Molecular Microbiology (2014) 92(3), 586–597 ■
doi:10.1111/mmi.12577
First published online 2 April 2014

The PAS domain-containing histidine kinase RpfS is a second sensor for the diffusible signal factor of *Xanthomonas campestris*

Shi-Qi An,[1] John H. Allan,[1] Yvonne McCarthy,[2] Melanie Febrer,[3] J. Maxwell Dow[2] and Robert P. Ryan[1]*

[1]*Division of Molecular Microbiology and* [3]*Division of Molecular Medicine, Colleges of Life Sciences, University of Dundee, Dundee, UK.*

[2]*School of Microbiology, Biosciences Institute, University College Cork, Cork, Ireland.*

Summary

A cell–cell signalling system mediated by the fatty acid signal DSF controls the virulence of *Xanthomonas campestris* pv. *campestris* (*Xcc*) to plants. The synthesis and recognition of the DSF signal depends upon different Rpf proteins. DSF signal generation requires RpfF whereas signal perception and transduction depends upon the sensor RpfC and regulator RpfG. Detailed analyses of the regulatory roles of different Rpf proteins have suggested the occurrence of further sensors for DSF. Here we have used a mutagenesis approach coupled with high-resolution transcriptional analysis to identify XC_2579 (RpfS) as a second sensor for DSF in *Xcc*. RpfS is a complex sensor kinase predicted to have multiple Per/Arnt/Sim (PAS) domains, a histidine kinase domain and a C-terminal receiver (REC) domain. Isothermal calorimetry showed that DSF bound to the isolated N-terminal PAS domain with a K_d of 1.4 μM. RpfS controlled expression of a sub-set of genes distinct from those controlled by RpfC to include genes involved in type IV secretion and chemotaxis. Mutation of *XC_2579* was associated with a reduction in virulence of *Xcc* to Chinese Radish when assayed by leaf spraying but not by leaf inoculation, suggesting a role for RpfS-controlled factors in the epiphytic phase of the disease cycle.

Accepted 10 March, 2014. *For correspondence. E-mail rpryan@dundee.ac.uk; Tel. (+44) 1382 386208; Fax (+44) 1382 388216.

Introduction

Phytopathogens belonging to the genus *Xanthomonas* cause diseases in many economically important plants throughout the world (Ryan and Dow, 2011; Ryan *et al*., 2011; Mansfield *et al*., 2012). These bacteria use cell–cell signalling mediated by molecules of the Diffusible Signal Factor (DSF) family to regulate expression of factors that contribute to virulence (Dow, 2008; Ryan and Dow, 2011; Ryan *et al*., 2011; Ryan, 2013). The DSF family of signals are *cis*-2-unsaturated fatty acids. DSF signalling was first described in the crucifer pathogen *Xanthomonas campestris* pv. *campestris* (*Xcc*) where the signal was identified as *cis*-11-methyl-2-dodecenoic acid (Wang *et al*., 2004; Ryan and Dow, 2011).

Work in *Xcc* has established that the synthesis and perception of the DSF signal require products of the *rpf* gene cluster (for regulation of pathogenicity factors). The synthesis of DSF is dependent on RpfF, which belongs to the crotonase superfamily of enzymes, whereas the RpfC/RpfG two-component system is implicated in DSF perception and signal transduction (Slater *et al*., 2000; Ryan *et al*., 2006; Ryan and Dow, 2011). RpfC is a complex hybrid sensor kinase whereas the RpfG regulator has a CheY-like receiver (REC) domain attached to an HD-GYP domain, which acts to degrade the second messenger cyclic di-GMP (Ryan *et al*., 2006; 2010; 2012).

Mutation of *rpfF*, *rpfG*, or *rpfC* in *Xcc* leads to a co-ordinate reduction in the synthesis of particular virulence factors such as the extracellular enzymes endoglucanase, protease, and endomannanase and the extracellular polysaccharide (EPS) xanthan, alterations in biofilm formation and a reduction in virulence (Slater *et al*., 2000; Dow *et al*., 2003; Ryan *et al*., 2006). Addition of DSF can restore the synthesis of these factors to *rpfF* mutants but not to *Xcc* strains with mutations in *rpfG* or *rpfC*. These findings are consistent with the involvement of RpfC/RpfG in perception and transduction of the DSF signal in a linear pathway (Slater *et al*., 2000; Ryan *et al*., 2006; 2012). However a recent study using RNA-Seq to compare the transcriptomes of wild-type and isogenic *rpf* mutants in *Xcc* has provided evidence for additional complexity in the

Rpf/DSF regulatory system (An *et al*., 2013). Accordingly, the regulatory influence of RpfF and RpfC demonstrate considerable overlap, but RpfF regulates transcript levels of 48 genes that are not regulated by RpfC and conversely RpfC regulates transcript levels of 135 genes that are not regulated by RpfF. These findings suggest that RpfC can recognize other environmental signals (in addition to DSF) and point to the possibility of alternative sensing mechanisms for DSF.

The aim of the work reported here was to identify alternative sensors for DSF in *Xcc*. Our approach was firstly to use comparative transcriptome analysis of wild-type, *rpfF*, *rpfC* and *rpfFC* double mutant strains to establish that a subset of genes are regulated by DSF but not by RpfC. Then, using one of these genes as a reporter, we performed a mutant screen in an *rpfFC* background to define a panel of transposon mutants that did not respond to exogenous DSF. One of these mutants carried a transposon insertion in *XC_2579*, which encodes a sensor kinase whose putative function in DSF signal transduction we have analysed in detail.

Results

Comparative transcriptomics of wild-type, rpfF, rpfC and rpfFC strains

Three independent cultures of each *Xcc* strain were subcultured and grown at 30°C to logarithmic phase (OD_{600} of 0.7–0.8) in NYGB broth without antibiotic selection. RNA was extracted from three technical replicates of each of the three biological replicates (for a total of nine samples) as described in *Experimental procedures*. After depletion of rRNA, barcoded cDNA libraries were generated and all samples were sequenced on an Illumina HiSeq2000. Read mapping, annotation and quantification of transcript levels were done as described in *Experimental procedures* (see Table S1).

Differential expression was assessed using Cufflinks (Trapnell *et al*., 2010; 2012). Cufflinks reports an expression value for each transcript and gene in Fragments Per Kilobase of exon model per Million mapped fragments (FPKM). Differentially expressed genes [with a fold change ≥ 3.0 and a stringent adjusted *P*-value (padj) of less than 0.1] along with their assigned annotations are listed for each mutant in Tables S2 and S3.

This transcriptome profile analysis revealed that expression of 107 genes was significantly altered by the inactivation of *rpfF*. Deletion of *rpfC* appeared to have a similar influence on global gene expression as 119 genes showed significantly altered expression in the mutant compared with wild-type (Fig. 1A and B). The major transcriptional changes reported here in *rpfF* and *rpfC* mutants were consistent with those reported in our previous study (An *et al*., 2013), although the parameters used for analysis in the two studies were different. RpfF and RpfC commonly regulated 79 genes, consistent with our earlier observations of the considerable overlap of the regulatory influences of these proteins. In marked contrast, analysis of the *rpfFC* mutant revealed 713 genes that were differentially expressed in comparison to the wild-type (Fig. 1A and B). These results suggest a strong synergy between the effects of RpfF and RpfC on gene expression.

Quantitative RT-PCR methods were used to confirm alterations in gene expression revealed by RNA-Seq. The genes selected for these analyses represented those with a range of fold change of expression and of diverse functional classes. The relative expression levels of the genes measured using qRT-PCR in each mutant reflected the differences in gene expression observed by transcriptome analysis (Fig. 1C). Importantly, known *Xcc* 8004 reference or housekeeping genes such as *gyrB*, *proC*, *recA*, *atpD* and *dnaK* were not differentially expressed between the wild-type and mutant samples. Of particular interest for the work described here is the panel of genes whose expression is altered in the *rpfF* and *rpfFC* mutants but not in the *rpfC* mutant. These genes represent candidates that are regulated by DSF but by a pathway that does not involve RpfC. One of these genes (*XC_0107*, encoding a hypothetical protein) was chosen as a reporter for a genetic screen to identify potential alternate sensors for DSF.

Genetic screen identifies XC2579 as a potential DSF sensor

A reporter for use in a genetic screen was constructed by cloning the promoter region of *XC_0107* into the GFP-based promoterless reporter plasmid pJBA23, as described in *Experimental procedures*. This reporter construct was transformed into the *rpfFC* strain. The expression of GFP by this transconjugant was activated by addition of DSF to the culture medium (Fig. 2A). A library of transposon mutants of this reporter strain was constructed using the Mariner transposon and was screened for loss of responsiveness to exogenous DSF (see *Experimental procedures*). Approximately 2000 mutants were screened with 42 mutants demonstrating altered levels of expression of the reporter fusion. PCR and nucleotide sequencing allowed the location of the transposon within the *Xcc* genome to be established for a number of these mutants (Table 1). The genes that were disrupted in these non-responsive mutants encode products with a range of different functions and a number of these are hypothetical proteins. However mutations in the majority of these genes are likely to have polar effects. In contrast, *XC_2579*, encoding a sensor kinase, is predicted to be monocistronic (Fig. 2B) and was therefore identified as a putative element in an alternate DSF signalling pathway (i.e. one that does not involve RpfC).

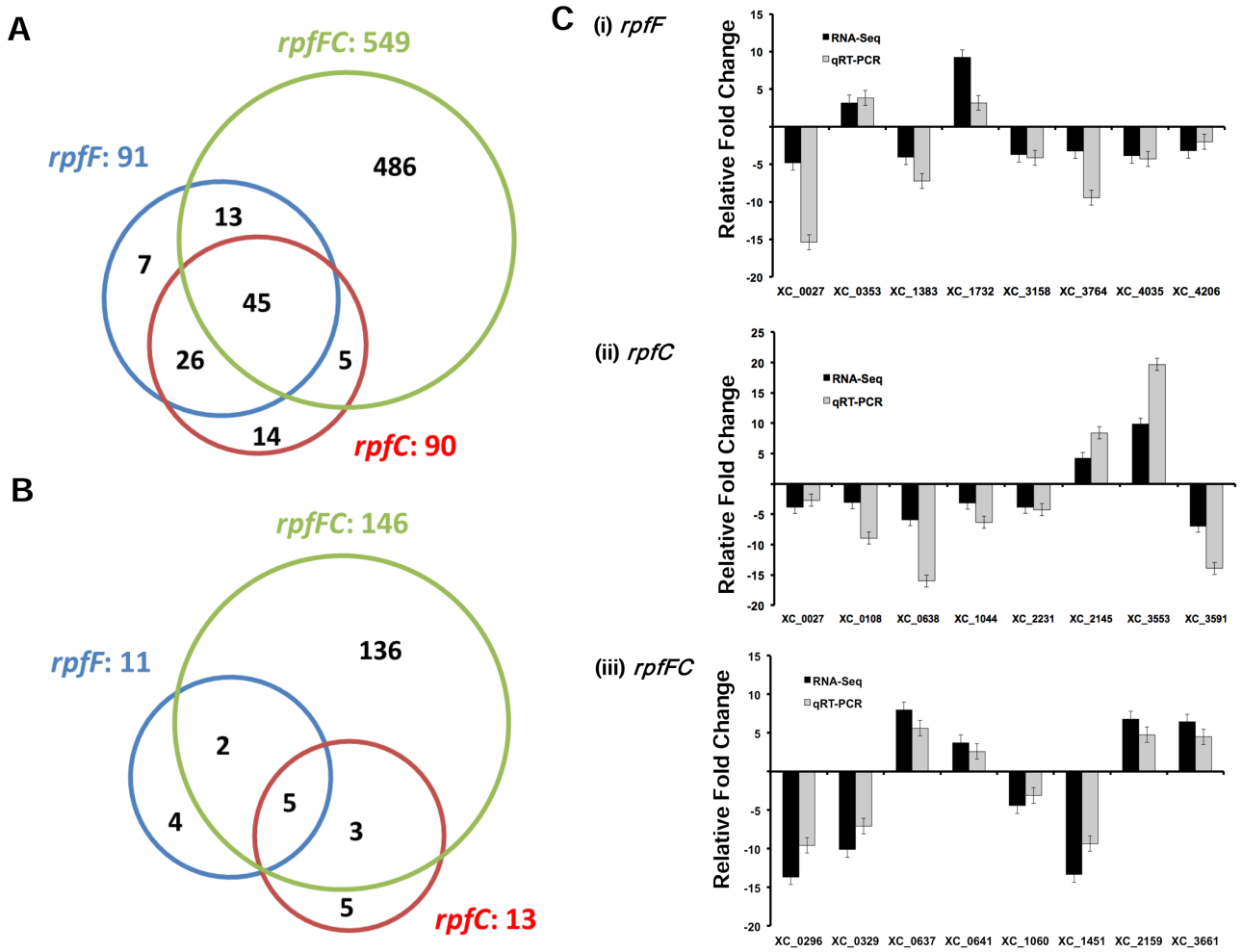

Fig. 1. Changes in gene expression of *rpfF*, *rpfC* and *rpfFC* mutants compared with the wild-type *Xcc* 8004 as measured by RNA-Seq.
A and B. Venn diagrams showing the overlap of genes whose expression is (A) downregulated or (B) upregulated in different mutant backgrounds. Divergently regulated genes are not depicted in these Venn diagrams but can be found in Table S3.
C. Comparison of relative fold changes between RNA-Seq and qRT-PCR results in (i) *rpfF*, (ii) *rpfC* and (iii) *rpfFC* mutant backgrounds. All qRT-PCR results were normalized using the *Ct*s obtained for the 16S rRNA amplifications run in the same plate. The relative levels of gene transcripts are determined from standard curves. Values given are the mean and standard deviation of triplicate measurements (three biological and three technical replicates).

To further examine this hypothesis, *Xcc* strains with a deletion of *XC_2579* in wild-type and *rpfFC* backgrounds were constructed as described in *Experimental procedures* and the expression of the *XC_0107 gfp* reporter in response to added DSF was measured. As found in the transposon mutant screen, deletion of *XC_2579* in the *rpfFC* background abrogated the response to DSF (Fig. 2A). Deletion of *XC_2579* in the wild-type background also prevented the response to DSF. Complementation restored the response to DSF to near wild-type (Fig. 2A). Taken together, these findings suggest that XC_2579 has a role in DSF signalling in a pathway that activates expression of *XC_0107* but that does not involve RpfC.

The SMART algorithm indicates that XC_2579 is a hybrid sensor kinase with both histidine kinase and receiver (REC) domains and a complex sensory input region comprising multiple Per/Arnt/Sim (PAS) and PAC domains (Fig. 2C). The protein has no predicted membrane-spanning regions and a predicted cytoplasmic location.

The sensing of DSF by XC2579 require the PAS_4 domain

The genetic screen establishes XC_2579 as an element in a DSF signalling pathway but does not indicate its precise role. A putative role as a direct sensor for DSF was first assessed by examination of the binding of DSF to full-length and truncated versions of the protein using Isothermal Titration Calorimetry (see *Experimental procedures*). The full-length protein (955 amino acids) bound DSF with

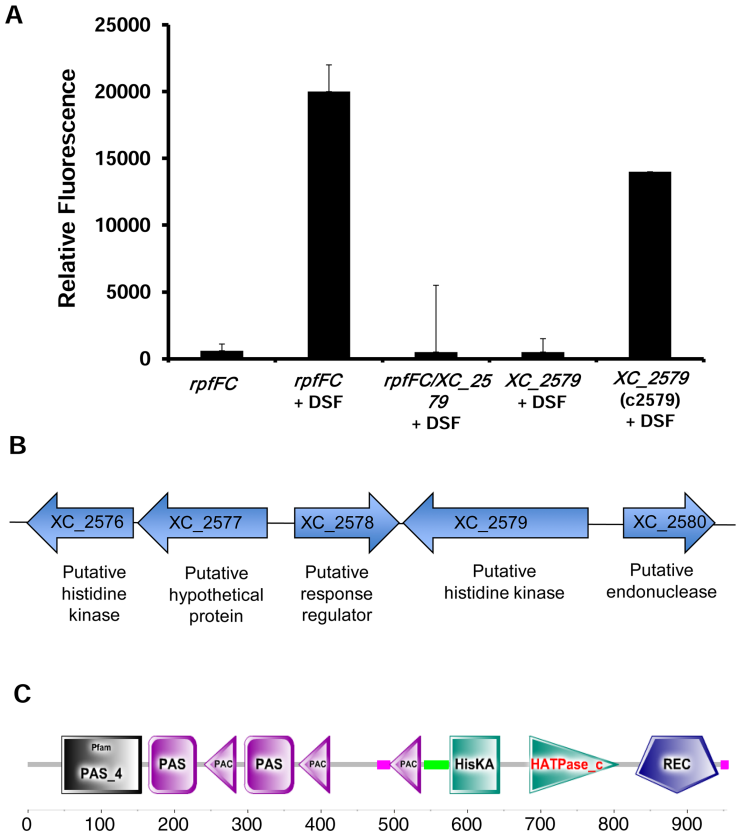

Fig. 2. DSF-induced expression of *XC_0107* and the role of XC_2579.
A. Effects of mutation of *XC_2579* in wild type and *rpfFC* mutant backgrounds on expression of *XC_0107 gfp* fusion induced by DSF. Bacteria carrying the promoter of *XC_0107* fused to *gfp* were grown overnight in NYGB medium at 30°C and subcultured (1:100) in fresh NYGB medium (5 ml) containing 50 μM synthetic DSF. The cells were grown at 30°C with shaking. After 14 h of cultivation, the GFP expression level was determined. Error bars show the standard deviation of triplicate experiments. Values observed are significant as they attain a *P*-value of less than 0.05.
(B) Genomic organization of the region encoding XC_2579 in *Xanthomonas campestris* 8004 and (C) domain structure of XC_2579 as revealed by the SMART algorithm (http://www.smart.embl-heidelberg.de).

high affinity (K_d of 1.4 μM) (Fig. 3B). A truncated derivative, Tk 1, comprising the N-terminal amino acid residues 1 to 360, also bound DSF with high affinity, although no binding was detected to Tk2, a derivative comprising amino acid residues 530–955. High affinity DSF binding was also seen to the Tk 3 and Tk 4 derivatives, proteins comprising amino residues 1 to 240 and 1 to 165 respectively of the full-length XC_2579. Tk 4 comprises just the N-terminal PAS_4 domain, suggesting that this is the site of DSF binding to full-length XC_2579.

Table 1. Location of transposon insertions found in the *Xanthomonas campestris* genome that lead to lack of responsiveness of *XC_0107* expression to exogenous DSF.

Disrupted gene[a]	Polar effect possible?[b]	Number of different transposon mutants[c]	Gene product
XC_0429	N	1	3-oxoacyl-ACP reductase
XC_0857	Y	1	Hypothetical protein
XC_0974	Y	1	Hypothetical protein
XC_1023	Y	1	Hypothetical protein
XC_1085	Y	1	Glutathione transferase
XC_1086	Y	1	GIY-YIG nuclease superfamily protein
XC_2247	Y	1	Flagellar protein
XC_2578	N	1	Response regulator
XC_2579	N	2	Histidine kinase/response regulator hybrid protein
XC_2644	Y	1	Chorismate mutase/prephenate dehydratase
XC_2979	Y	1	Enoyl-CoA hydratase
XC_3079	Y	1	DNA repair protein
XC_4035	Y	1	Hypothetical protein
XC_4143	Y	1	Hypothetical protein

a. None of these gene disruptions affect bacterial growth in complex or minimal media.
b. Possibility of transposon insertion affecting expression of other (downstream) genes. Y: yes; N: no.
c. Number of different independent transposon insertion mapped to the same gene.

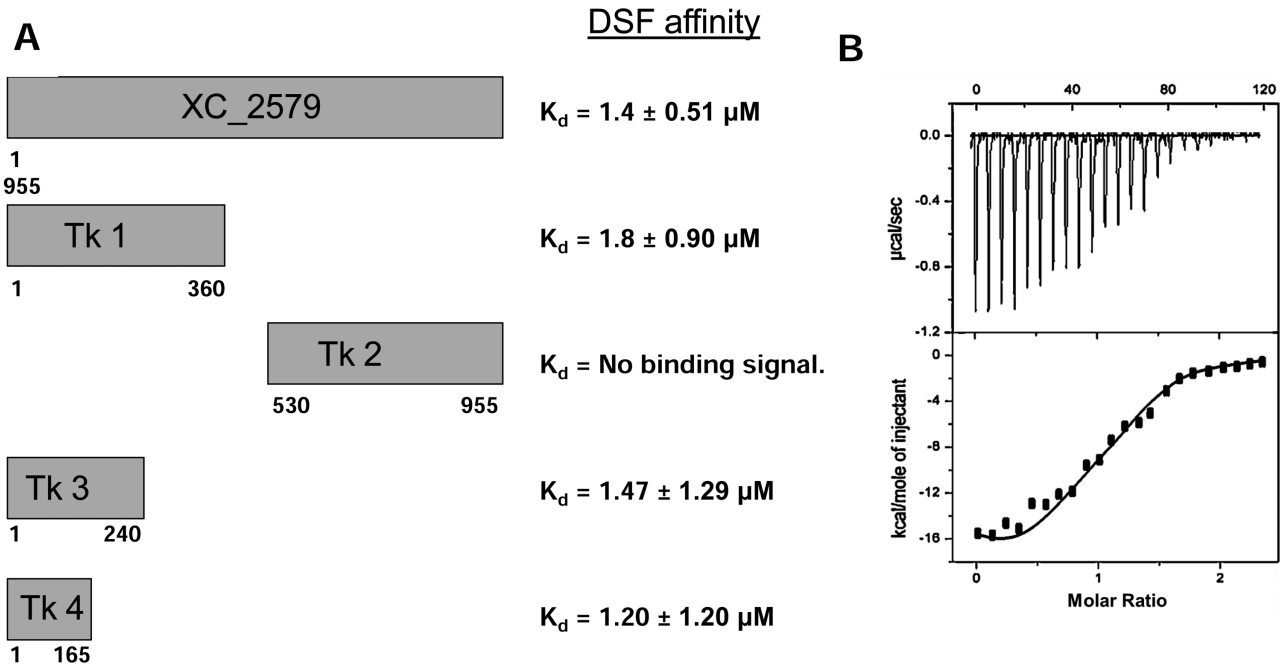

Fig. 3. Isothermal titration calorimetry analysis (ITC) of the interaction between DSF and XC_2579.
A. Summary of the binding affinity of full-length XC_2579 and truncations to DSF as derived by ITC.
B. A representative ITC data plot for titration of 20 μM of the PAS domain from XC_2579 (Tk 4) with 20 or 200 μM DSF in PBS buffer at 25°C.

The binding affinity of Tk4 for structural analogues of DSF (which is *cis*-11-methyl-2-dodecenoic acid) was then examined. The findings (Table 2) indicate that Tk 4 bound *cis*-2-dodecenoic acid (BDSF) with a slightly lower affinity than DSF (K_d of 7 μM), but had substantially reduced affinities for *trans*-11-methyl-2-dodecenoic acid and the saturated fatty acids 11-methyl-dodecanoic acid and dodecanoic acid (all K_d values > 1 mM). Thus Tk4 and by extension XC_2579 exhibits specificity for binding fatty acids of the DSF family over analogues that are not active in signalling in *Xcc*.

Mutation of XC2579 has broad effects on the Xcc transcriptome

The regulatory role of XC_2579 was then examined through comparative transcriptome profiling of the wild-type and an *XC_2579* deletion mutant using RNA-seq.

Table 2. Binding affinities of the N-terminal PAS domain from XC_2579 (Tk 4) with DSF and structural analogues determined by ITC.

Fatty acid ligand	Structure	K_d (M)	△H (kcal mol^{-1})	△S (cal mol^{-1} per degree)	ΔG (kcal mol^{-1})
cis-11-methyl-2-dodecenoic acid (DSF)	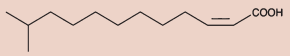	1.20×10^{-6} (± 0.5)	–1.60	59.73	–3.38
cis-2-dodecenoic acid (BDSF)	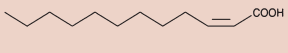	7.10×10^{-6} (± 1.3)	–1.21	58.05	–2.94
trans-11-methyl-2-dodecenoic acid	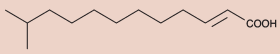	11.30×10^{-4} (± 2.4)	ND	ND	ND
11-methyl-dodecanoic acid	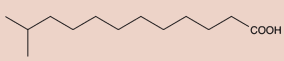	6.90×10^{-3} (± 1.0)	ND	ND	ND
Dodecanoic acid	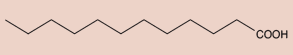	14.90×10^{-3} (± 3.7)	ND	ND	ND

K_d is the dissociation constant. ΔH, ΔS and ΔG are the change in enthalpy, entropy and Gibbs free energy upon binding. Binding not detected (ND) using the similar concentrations to DSF or BDSF. Higher concentrations of analogues were used to estimate K_d (thermodynamic characteristics not reported).

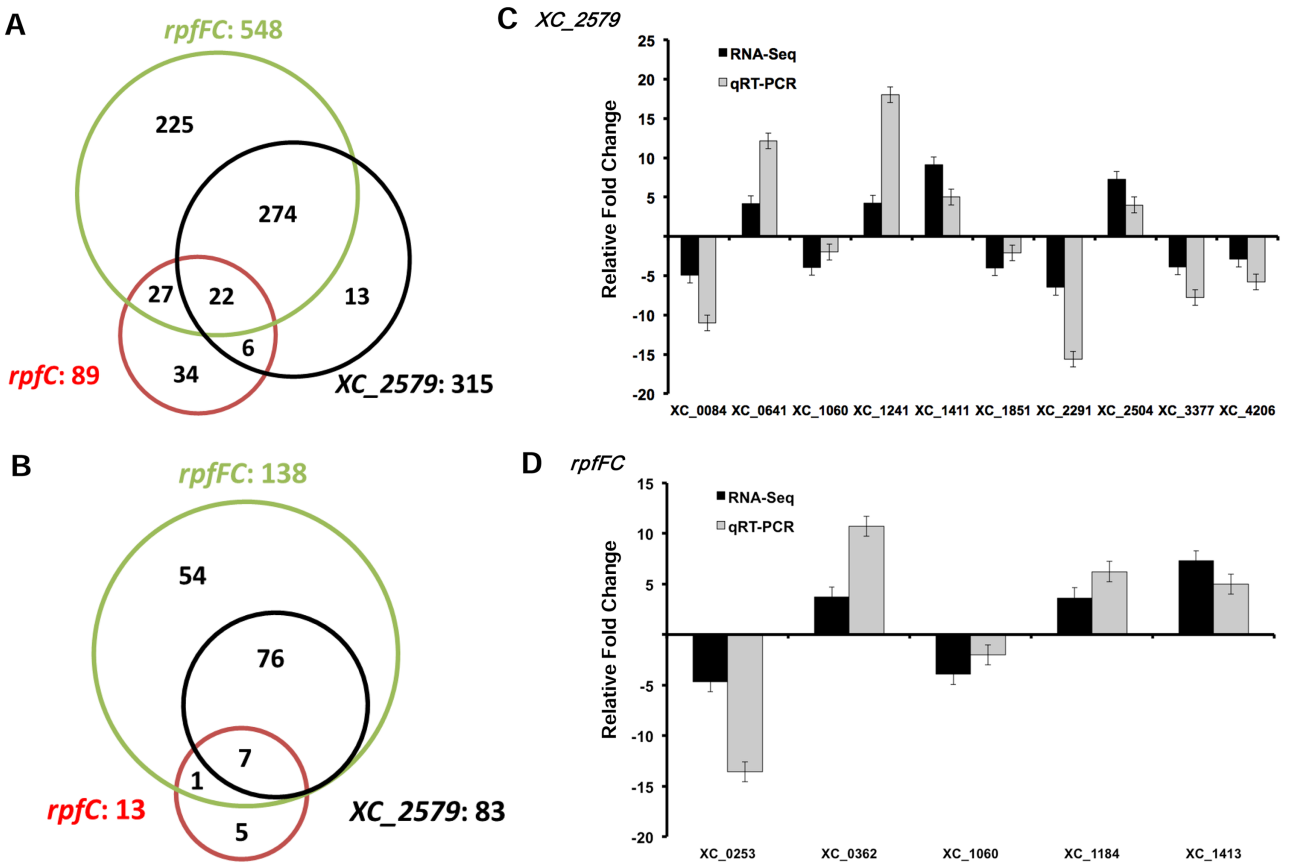

Fig. 4. Changes in gene expression of *rpfC*, *rpfFC* and *XC_2579* mutants compared with the wild-type *Xanthomonas campestris* 8004 as measured by RNA-Seq. Venn diagrams showing the overlap of genes whose expression is (A) downregulated or (B) upregulated in different mutant backgrounds. Divergently regulated genes are not depicted in these Venn diagrams but can be found in Table S3. Comparison of relative fold changes between RNA-Seq and qRT-PCR results in XC_*2579* mutant (C) and *rpfFC* mutant (D) background. All qRT-PCR results were normalized using the *Cts* obtained for the 16S rRNA amplifications run in the same plate. The relative levels of gene transcripts are determined from standard curves. Values given are the mean and standard deviation of triplicate measurements (three biological and three technical replicates).

Mutation of *XC_2579* had a broad effect on the transcriptome, significantly influencing the expression of 424 genes (Fig. 4A and B). Genes that are regulated are associated with diverse functions that include chemotaxis and type IV secretion (Table S3). Quantitative RT-PCR methods were used to confirm alterations in expression of selected genes as revealed by RNA-Seq. The relative expression levels of the genes measured using qRT-PCR in the *XC_2579* mutant reflected the differences in gene expression observed by transcriptome analysis (Fig. 4C and D). Comparative transcriptome analysis revealed that 352 of the genes whose expression was controlled by XC_2579 were also altered in the *rpfFC* mutant but not in the *rpfC* mutant (Fig. 4 A and B). These findings support the contention that XC_2579 is involved in a regulatory pathway that involves DSF but not RpfC.

Mutation of XC2579 influences motility and virulence in Xcc

The role of DSF signalling in controlling a range of factors that contribute to the virulence of *Xcc* is now well established (Slater *et al.*, 2000; Dow *et al.*, 2003; Ryan *et al.*, 2007; O'Connell *et al.*, 2013; Ryan, 2013). The role of XC_2579 as a sensor for DSF with a broad effect on the transcriptome prompted an analysis of the influence of mutation of *XC_2579* on expression of virulence factors and virulence. Mutation of *XC_2579* had no effect on the synthesis of extracellular enzymes such as endoglucanase, mannanase and protease or biofilm formation in L medium (data not shown). Notably, these functions are regulated by DSF but through a pathway involving RpfC. Mutation of *XC_2579* (or *rpfF*) affected motility of *Xcc* (Fig. 5A). Complementation with a clone expressing the

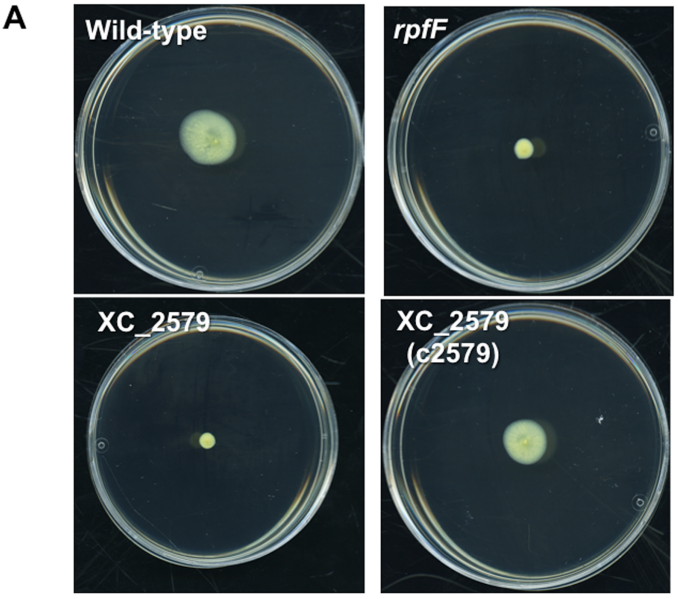

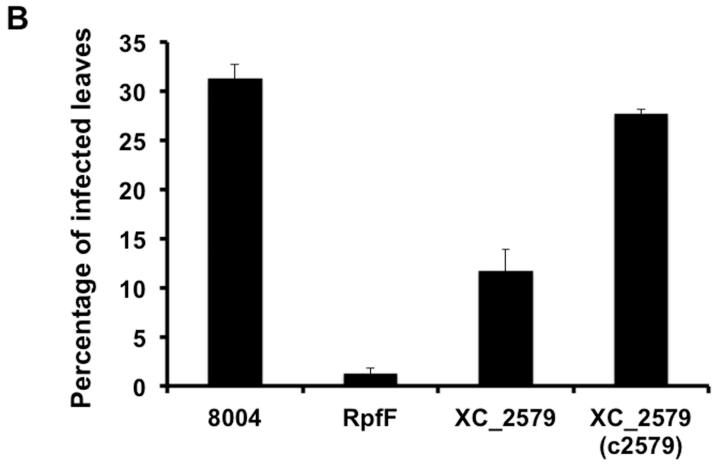

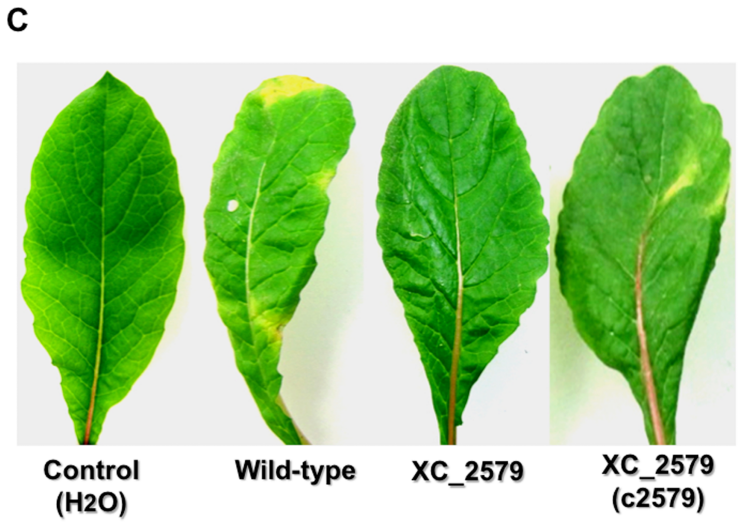

Fig. 5. Effect of mutation of *XC_2579* on motility and virulence in *Xcc*.
A. The motility of different *Xcc* strains was tested on Eiken agar. The *XC_2579* strain had reduced motility (comparable to the *rpfF* mutant). Motility was restored in the complemented strain XC_2579 (c2579).
B. Virulence of different *Xcc* strains assessed after spray inoculation. The percentage of the total number of inoculated leaves that showed the typical black rot disease symptoms at the leaf margin is given. Values are means and standard deviations of three replicates, each comprising 25 plants and approximately 100 leaves. Values observed are significant as they attain a *P*-value of less than 0.05.
C. Symptom production on leaves after 10 day spray inoculation with (from left to right) water (control), wild-type, XC_*2579* mutant and complemented strain XC_2579 (c2579).

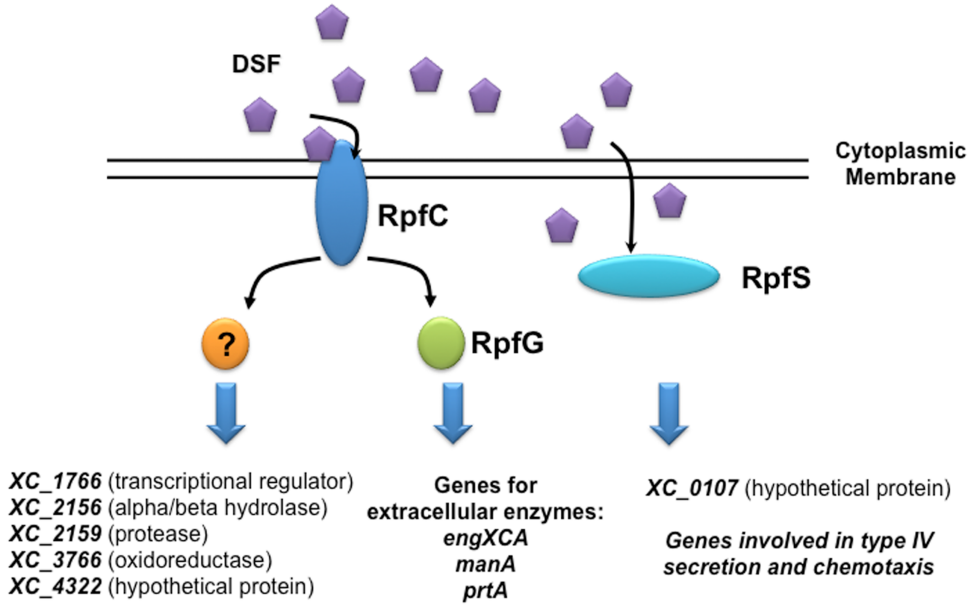

Fig. 6. Model for multiple pathways of DSF perception and signal transduction in *Xanthomonas campestris*. DSF perception and signal transduction involving the sensor RpfC and response regulator RpfG act to co-ordinately regulate the expression of a sub-set of genes that include *engXCA*, *prtA* and *manA*, which encode extracellular enzymes. DSF and RpfC also regulate expression of a number of genes including *XC_1766* (encoding a transcriptional regulator) independently of RpfG, suggesting further signalling outputs from RpfC. The second DSF-dependent sensor RpfS (XC_2579) regulates genes including *XC_0107* (encoding a hypothetical protein) in a pathway that is independent of RpfC and RpfG. Not depicted in the current model is the sub-set of genes co-regulated by RpfC and RpfS (XC_2579). How these genes are directly regulated is currently under investigation.

full length XC_2579 protein restored motility of the *XC_2579* mutant to wild-type levels. In contrast, complementation of XC_*2579* mutant with a clone expressing XC_2579 lacking the N-terminal PAS domain was unable to restore motility (Fig. S1). Western analysis with an anti-His6 antiserum showed that the N-terminally truncated XC_2579 protein was however expressed in *Xcc.* These observations suggest DSF can regulate motility through a pathway or pathways involving XC_2579.

We have previously shown that the *rpfF* (and *rpfC*) mutants show considerably reduced virulence in Chinese Radish when plants are inoculated by leaf clipping (Dow *et al*., 2003; Ryan *et al*., 2007; An *et al*., 2013). The *XC_2579* mutant showed no reduction in virulence when this method of inoculation was used (data not shown). However when plants were inoculated by spraying (see *Experimental procedures*), both *rpfF* and *XC_2579* mutants showed reduced virulence, as indicated by a reduction in the percentage of inoculated leaves that develop black rot symptoms (Fig. 5B and C). The effect of *XC_2579* mutation on virulence was less pronounced than that of *rpfF* mutation however. Complementation of the *XC_2579* mutant restored virulence to near wild-type level (Fig. 5B and C). These findings suggest a role for DSF signalling and XC_2579 in the epiphytic phase of the *Xcc* disease cycle.

Discussion

The PAS domain and fatty acid signals

The findings represent the second report implicating the PAS domain in sensing cell–cell signals of the DSF family in bacteria (Fig. 6). RpfR from *Burkholderia cenocepacia* is a sensor for BDSF in which a PAS domain is linked to GGDEF and EAL domains that are implicated in cyclic di-GMP turnover (Deng *et al*., 2012). Notably, the N-terminal PAS domain of XC_2579 (RpfS) has much lower affinity for the *trans*-isomer of DSF or saturated fatty acids lacking the *cis* double bond at the 2-position, molecules that have little or no activity in DSF signalling. The binding of fatty acids by a PAS domain has been reported previously (King-Scott *et al*., 2011). Palmitoleic acid and oleic acid have been shown to bind to the PAS domain of *Mycobacterium tuberculosis* Rv1364c, a multidomain protein which regulates the activity of the stress-dependent σ factor, σ(F). The PAS domain of Rv1364c also binds palmitic acid but with 100 times lower affinity than for palmitoleic acid. Whether fatty acid binding has a role in modulation of Rv1364c activity is as yet unclear.

This report and the previous report of RpfR in *B. cenocepacia* add to a growing body of work that reflects the diversity of protein domains involved in DSF sensing in different bacteria. Sensory input domains similar to that of

RpfC are found in other proteins such as the histidine kinase PA1396 of *Pseudomonas aeruginosa*, which is implicated in interspecies signalling mediated by DSF. However the sensory input domain of the histidine kinase BCAM0227, the first BDSF sensor described in *B. cenocepacia*, is quite different from RpfC (McCarthy *et al*., 2010; Ryan and Dow, 2011). None of these sensory domains resemble a PAS domain.

The expansion of classes of receptor to include the PAS domain opens up the possibility that the number of species capable of DSF family-mediated intraspecies or interspecies signalling may also expand beyond those already identified or predicted. Thus far we have relied on the presence of linked genes (*rpfFCG* genes as in *Xcc* or *rpfFR* as in *B. cenocepacia*) to predict the occurrence of intraspecies DSF signalling in an organism and the presence of input domains similar to RpfC or Bcam0227 to identify putative interspecies signalling elements. However predictions of the existence of DSF signalling systems involving PAS domain proteins in other bacteria may not be straightforward, since the PAS domains of XC_2579 and RpfR lack significant sequence similarity. Additionally, those proteins of the crotonase superfamily that are specifically DSF synthases cannot as yet be identified by bioinformatics.

Homologues of RpfS in other xanthomonads

BLASTP searches indicate that homologues of RpfS occur in a number of additional *Xanthomonas* species (to include *X. citri*, *X. axonopodis* and *X. euvesicatoria*) but are apparently absent from *Xanthomonas* species attacking monocots such as *X. oryzae* and *X. translucens*. Similarly an RpfS homologue is found in *Stenotrophomonas* strain SKA14 but not in *S. maltophilia* R-551 or K279a. There is no homologue in *Xylella*.

RpfS and the virulence of Xcc

Mutation of *XC_2579* has no effect on the virulence of *Xcc* when the bacteria are introduced into the leaf vascular system by leaf clipping, but does influence virulence when bacteria are sprayed onto the leaves of intact plants. Under these latter conditions, bacteria are required to move towards the preferred portal of entry, which is the hydathode at the leaf margin, and then enter the vascular system of the plant. The reduced expression of genes involved in chemotaxis and the reduced motility of the *XC_2579* mutant may in part contribute to this reduced virulence. Whether other functions under XC_2579 regulation have any influence on virulence when assayed by spraying is not known. For example, the role of type IV secretion in *Xanthomonas* spp. is currently unclear.

Signal transduction involving RpfS

The occurrence of multiple PAS domains in XC_2579 suggests that this protein can sense multiple environmental or cellular signals. This may explain the observation that a number of the genes that are regulated by XC_2579 (for example those involved in type IV secretion) do not have a significantly altered expression in the *rpfF* mutant (see Fig. 6). In this case, other environmental inputs into the XC_2579 sensor may act to control this and other functions in the *rpfF* mutant background.

As shown in Fig. 2C, XC_2579 is a hybrid kinase with both histidine kinase and REC domains, but lacking the C-terminal Hpt domain found in other hybrid kinases such as RpfC. This domain arrangement is not uncommon in *Xcc*, as there are 16 examples of histidine kinases with a REC but no HPt domain encoded by the *Xcc* genome. In other bacteria such as *Pseudomonas aeruginosa*, stand-alone Hpt domain proteins act downstream of such sensor kinases in signal transduction cascades. However the *Xcc* genome does not encode any stand-alone Hpt domain proteins; there are 7 HPt domain-containing proteins but all are histidine kinases. The mutagenesis study (Table 1) suggested a role of XC_2578 in the response of the *rpfFC* mutant to added DSF. *XC_2578* is convergently transcribed to *XC_2579* and encodes a 124 amino acid protein comprising a stand-alone REC domain with a potential phosphorylation site at the aspartate residue 59. Further work is needed to investigate any interplay between XC_2579 and XC_2578 in relation to DSF signal transduction.

Concluding remarks

The description of RpfS as a DSF sensor in *Xcc* (this work) and of RpfR as a BDSF sensor in *B. cenocepacia* (Deng *et al*., 2012) indicates that each of these bacteria has two receptors for the same family of signal molecule. The available evidence indicates that both *Xcc* receptors (RpfC and RpfS) recognize DSF preferentially over BDSF, whereas the two *B. cenocepacia* receptors (RpfR and Bcam0227) recognize BDSF in preference to DSF. It is possible however that differences in affinity or specificity for different DSF family members (that vary in chain length or branching) occur. Although the detailed mechanisms are different, there are a number of intriguing parallels in DSF signalling between these organisms. Each bacterium links perception of a DSF family signal to alteration in cyclic di-GMP by a system that is encoded by a gene or genes linked to the signal synthase gene. In addition, each organism has a genetically unlinked two-component sensor that serves to regulate expression of a distinct subset of genes under cell–cell signalling control. Finally each organism has a sensor that is located at the cytoplasmic membrane

and one that is probably soluble in the cytoplasm. Despite these broad parallels, the appreciation of the existence of multiple and diverse receptors for DSF family signals means that we are still some way from understanding DSF signalling in any one organism or indeed the scope of DSF signalling in the wider microbial world.

Experimental procedures

Bacterial strains and growth conditions

The wild-type *Xanthomonas campestris* pv. *campestris* (*Xcc*) 8004 and other strains have been described previously (An *et al*., 2013). In-frame deletion of selected genes was carried out using pK18*mobsac* as described previously (Slater *et al*., 2000). All plasmids and strains used during this study are described in Table S4. For most experiments, *Xcc* strains were grown in NYGB medium, which comprises 5 g l^{-1} bacteriological peptone (Oxoid), 3 g l^{-1} yeast extract (Difco), and 20 g l^{-1} glycerol. The antibiotics used were kanamycin (Km), rifampicin (Rif), gentamicin (Gm), spectinomycin (Sp) and tetracycline (Tc); the concentrations used are indicated.

DNA manipulation

Molecular biological methods such as isolation of plasmid and chromosomal DNA, PCR, plasmid transformation as well as restriction digestion were carried out using standard protocols (Sambrook *et al*., 1989). PCR products were cleaned using the Qiaquick PCR purification kit (Qiagen) and DNA fragments were recovered from agarose gels using Qiaquick minielute gel purification kit (Qiagen). Oligonucleotide primers were purchased from Sigma-Genosys.

RNA extraction and preparation

Three independent cultures of each selected *Xanthomonas* strain were subcultured and grown to logarithmic phase (0.7–0.8 OD_{600}) at 30°C in NYGB broth without selection. 800 µl of RNA protect (Qiagen) was added to 400 µl culture and incubated at room temperature for 5 min. Cell suspensions were centrifuged, the supernatant was discarded, and pellets were stored at −80°C. After thawing, 100 µl TE-lysozyme (400 µg ml^{-1}) was added and samples were incubated at room temperature. Total RNA was isolated using the RNeasy Mini Kit (Qiagen) whereby cells were homogenized utilizing a 20-gauge needle and syringe. Samples were treated with DNase (Ambion) according to manufacturer's instructions and the removal of DNA contamination was confirmed by PCR.

Library construction and cDNA sequencing

RNA quality was assessed on a Bioanalyser PicoChip (Agilent) and RNA quantity was measured using the RNA assay on QuBit fluorometer (Life Technologies). Ribosomal RNA was depleted with Ribo-Zero™ rRNA Removal Kits for Gram-Negative Bacteria (Epicentre). The percentage of rRNA contamination was checked on a Bioanalyser PicoChip (Agilent).

The rRNA-depleted sample was processed using the Illumina TruSeq RNA v2 sample preparation kit. In brief, the sample was chemically fragmented to ~ 200 nt in length and the cleaved RNA fragments were primed with random hexamers into first strand cDNA using reverse transcriptase and random primers. The RNA template was removed and a replacement strand was synthesized to generate ds cDNA. The ds cDNA was end repaired to remove the overhangs from the fragmentation into blunt ends. A single 'A' nucleotide was added to the 3′ ends on the blunt fragments, which is complementary to a 'T' nucleotide on the 3′ end of the Illumina adapters. At this stage, adapters containing 6 nt barcodes were used for different samples to allow the pooling of multiple samples together. The resulted barcoded samples were enriched by 10 cycles of PCR to amplify the amount of DNA in the library. The final cDNA libraries were sequenced on an Illumina HiSeq2000 as per manufacturer's instructions. The RNA-Seq raw data files are accessible through XanthomonasGbrowse: http://browser.bbsrc.ac.uk/cgi-bin/gb2/gbrowse/Xanthomonas.

Computational analysis

Cluster generation was performed using the Illumina cBot and the cDNA fragments were sequenced on the Illumina HiSeq2000 following a standard protocol. The fluorescent images were processed to sequences using the Pipeline Analysis software 1.8 (Illumina). Raw sequence data obtained in Illumina FASTQ-format were first separated by their barcode sequence by comparing the first 6 bases with the expected barcode sequences. Successfully detected barcodes were removed from the sequence leaving reads of 30 nt in length, while reads containing no recognizable barcode sequence were discarded.

Read mapping, annotation and quantification of transcript levels

Reads for each sample were aligned to the *Xanthomonas campestris* pv. *campestris* 8004 NC_007086 assembly [Integrated Microbial Genomes (IMG) database, taxon object ID 637000343] using Bowtie version 0.12.7 with default parameters. Transcript abundance was determined for the gene models annotated in the IMG *Xanthomonas campestris* pv. *campestris* 8004 genome release IMG/W 2.0 using the Bowtie RNA-Seq BAM alignments for each of the samples. To estimate the level of transcription for each gene, the number of reads that mapped within each annotated coding sequence (CDS) was determined. Related servers RAST (Aziz *et al*., 2008) and Prodigal (Hyatt *et al*., 2010) were also used in this way.

Analysis of differential expression

Differential expression was assessed using Cufflinks (Trapnell *et al*., 2010; 2012). Cufflinks reports an expression value for each transcript and gene in Fragments Per Kilobase of exon

model per Million mapped fragments (FPKM). A test statistic is also calculated, after Benjamini-Hochberg correction for multiple-testing was used to determine significant changes in expression between each pair of samples (false discovery rate 0.05). A stringent padj was set at of less than 0.1.

Quantitative real-time PCR

Quantitative RT-PCRs were used to validate RNA-Seq data. Reverse transcription PCR was achieved using a cDNA synthesis kit (Promega) according to the manufacturer's instructions. Specific RT-PCR primers were used to amplify central fragments of approximately 200 bp in length from different genes. Semi-quantitative RT-PCRs were completed using 250 ng μl^{-1} cDNA template and PCR Mastermix (Promega) for 24–36 cycles. For qRT-PCRs, quantification of gene expression and melting curve analysis were completed using a LightCycler (Roche) and Platinum SYBR Green qPCR Supermix-UGD (Invitrogen) was used according to manufacturer's instructions. The constitutively expressed housing keeping gene, *16S rRNA* was used as a reference to standardize all samples and replicates.

Construction of XC_0107gfp reporter fusion

Using the genome sequence of *Xcc* 8004 (http://cmr.tigr.org), the promoter region of *XC_0107* comprising the region 250 bp upstream of the gene was amplified by PCR using forward and reverse primers 0105-F (5′–3′) and 0105-R (5′–3′). This fragment was cloned into a GFP-based promoterless reporter plasmid pJBA23 (Rybtke *et al*., 2012). The *XC_0107*::*GFP* fusion plasmid above was then transferred into the *Xcc* 8004 wild-type or *rpfFC* mutant, thus generating 8004/*XC_0107*::*GFP* and *rpfFC*/*XC_0107*::*GFP* (Table S4).

Transposon mutagenesis and screening

A library of mutants in the *rpfFC* strain carrying the *XC_0107*::*GFP* fusion was constructed using Mariner transposon vector pBT20 as previously described (Kulasekara *et al*., 2005). Briefly, 100 ng of transposon-containing plasmid was electroporated into newly prepared electrocompetent *rpfFC* mutant cells. Strains carrying the transposon insertion were identified by selection on Gm. The library of mutants was screened for loss of responsiveness of *XC_0107*::*GFP* expression to exogenous DSF. Strains were inoculated into microtitre wells containing LB medium with 250 nmol DSF by using a Qpix robot (Genetix™). The fluorescence of bacteria from each well was quantified as described previously (McCarthy *et al*., 2010). Briefly, equal amounts of bacterial cells as adjusted by determination of optical density at 600 nm (OD_{600}) of the cultures were screened via flow cytometry and on a fluorescence plate reader (Bio-Tek FL600; Bio-Tek Instruments, Winooski, VT).

Identification of sites of transposon insertion

Genomic DNA was extracted from transposon mutants of interest as previously described (Sambrook *et al*., 1989). The nucleotide sequence flanking the transposon insertion site was amplified by PCR as previously described (McCarthy *et al*., 2010) using the primers: Rnd1-TnM and Rnd2-TNm. Amplicons were sequenced using the TnM specific primer: TnMseq. Sequence data generated were examined with BLASTn, BLASTx (http://www.ncbi.nlm.nih.gov/BLAST/), and VGE BLAST (http://www.vge.ac.uk/BLAST/) software.

Protein expression and purification

The DNA fragments encoding the full-length XC_2579 protein and the truncated derivatives were synthesized by Gene Oracle in pGOv4 and subcloned into pET47b before transformation into *E. coli* BL21 (DE3). BL21 (DE3) cells were grown in LB media and induced with 0.25 mM IPTG; protein overexpression was carried out at 37°C for 1 h. Purification was achieved by Ni^{2+} affinity chromatography using the N-terminal His6 tag followed by tag cleavage using recombinant HRV 3C protease.

Isothermal titration calorimetry

The isothermal titration calorimetry (ITC) measurements were obtained using a VP-ITC microcalorimeter following the manufacturer's protocol (MicroCal, Northampton, MA). In brief, titrations began with one injection of 2 μl of DSF (20 or 200 μM) solution into the sample cell containing 1.4 ml of XC_2579 (or truncation) solution (20 μM) in the VP-ITC microcalorimeter. The volume of DSF or analogues injection was changed to 10 μl in the subsequent twenty-eight injections. The heat changes accompanying injections were recorded. The titration experiment was repeated at least twice, and the data were calibrated with a buffer control and fitted with the one-site model to determine the binding constant (K_d) using the MicroCal ORIGIN version 7.0 software.

Phenotypic analysis

All phenotypic assays of *Xcc* strains used in this study have been described previously (Ryan *et al*., 2010; An *et al*., 2013). Activities of the extracellular enzymes β-1,4-endoglucanase and β-1,4-mannanase in culture supernatants were estimated by radial diffusion assays into substrate-containing plates by using locust bean gum (Sigma) and carboxymethylcellulose. Motility was assayed as described previously on NYGB solidified with 0.5% Eiken agar (Eiken Chemical, Tokyo).

Virulence assays

Virulence of *Xcc* strains to Chinese radish (*Raphanus sativus*) was examined by spraying assay. For this assay five-week old seedlings with fully expanded leaves were used. Bacteria were grown overnight in NYGB medium, centrifuged and re-suspended in water to a cell density OD of 0.01 at 600 nm for spraying. A volume of 50 ml of the bacterial suspension was inoculated onto the leaves of 25 plants (approximately 100 leaves) by spraying. Three replicates of each independent experiment were carried out. Ten days

after inoculation the relative virulence was determined as the percentage of the total inoculated leaves that showed the typical black rot disease symptoms at the leaf margin. The experiment was repeated three times.

Acknowledgements

The work of the authors has been supported in part by grants awarded by the Wellcome Trust WT093314MA to J.M.D. and R.P.R. and WT100204AIA senior fellowship grant to R.P.R.; the Science Foundation Ireland (SFI 07/IN.1/B955 to J.M.D. and SFI 09/SIRG/B1654 to R.P.R.).

References

An, S.Q., Febrer, M., McCarthy, Y., Tang, D.J., Clissold, L., Kaithakotti, G., *et al*. (2013) High-resolution transcriptional analysis of the regulatory influence of cell-to-cell signalling reveals novel genes that contribute to *Xanthomonas* phytopathogenesis. *Mol Microbiol* **88:** 1058–1069.

Aziz, R.K., Bartels, D., Best, A.A., DeJongh, M., Disz, T., Edwards, R.A., *et al*. (2008) The RAST server: rapid annotations using subsystems technology. *BMC Genomics* **9:** e75.

Deng, Y., Schmid, N., Wang, C., Wang, J., Pessi, G., Wu, D., *et al*. (2012) Cis-2-dodecenoic acid receptor RpfR links quorum-sensing signal perception with regulation of virulence through cyclic dimeric guanosine monophosphate turnover. *Proc Natl Acad Sci USA* **109:** 15479–15484.

Dow, J.M., Crossman, L., Findlay, K., He, Y.Q., Feng, J.X., and Tang, J.L. (2003) Biofilm dispersal in *Xanthomonas campestris* is controlled by cell–cell signaling and is required for full virulence to plants. *Proc Natl Acad Sci USA* **100:** 10995–11000.

Dow, M. (2008) Diversification of the function of cell-to-cell signaling in regulation of virulence within plant pathogenic xanthomonads. *Sci Signal* **1:** pe23.

Hyatt, D., Chen, G.-L., LoCascio, P.F., Land, M.L., Larimer, F.W., and Hauser, L.J. (2010) Prodigal: prokaryotic gene recognition and translation initiation site identification. *BMC Bioinformatics* **11:** 119.

King-Scott, J., Konarev, P.V., Panjikar, S., Jordanova, R., Svergun, D.I., and Tucker, P.A. (2011) Structural characterization of the multidomain regulatory protein Rv1364c from *Mycobacterium tuberculosis*. *Structure* **19:** 56–69.

Kulasekara, H.D., Ventre, I., Kulasekara, B.R., Lazdunski, A., Filloux, A., and Lory, S. (2005) A novel two-component system controls the expression of *Pseudomonas aeruginosa* fimbrial *cup* genes. *Mol Microbiol* **55:** 368–380.

McCarthy, Y., Yang, L., Twomey, K.B., Sass, A., Tolker-Nielsen, T., Mahenthiralingam, E., *et al*. (2010) A sensor kinase recognizing the cell–cell signal BDSF (cis-2-dodecenoic acid) regulates virulence in *Burkholderia cenocepacia*. *Mol Microbiol* **77:** 1220–1236.

Mansfield, J., Genin, S., Magori, S., Citovsky, V., Sriariyanum, M., Ronald, P., *et al*. (2012) Top 10 plant pathogenic bacteria in molecular plant pathology. *Mol Plant Pathol* **13:** 614–629.

O'Connell, A., An, S.Q., McCarthy, Y., Schulte, F., Niehaus, K., He, Y.Q., *et al*. (2013) Proteomics analysis of the regulatory role of Rpf/DSF cell-to-cell signaling system in the virulence of *Xanthomonas campestris*. *Mol Plant Microbe Interact* **26:** 1131–1137.

Ryan, R.P. (2013) Cyclic di-GMP signalling and the regulation of bacterial virulence. *Microbiology* **159:** 1286–1297.

Ryan, R.P., and Dow, J.M. (2011) Communication with a growing family: diffusible signal factor (DSF) signaling in bacteria. *Trends Microbiol* **19:** 145–152.

Ryan, R.P., Fouhy, Y., Lucey, J.F., Crossman, L.C., Spiro, S., He, Y.W., *et al*. (2006) Cell–cell signaling in *Xanthomonas campestris* involves an HD-GYP domain protein that functions in cyclic di-GMP turnover. *Proc Natl Acad Sci USA* **103:** 6712–6717.

Ryan, R.P., Fouhy, Y., Lucey, J.F., Jiang, B.-L., He, Y.-Q., Feng, J.-X., *et al*. (2007) Cyclic di-GMP signaling in the virulence and environmental adaptation of *Xanthomonas campestris*. *Mol Microbiol* **63:** 429–442.

Ryan, R.P., McCarthy, Y., Andrade, M., Farah, C.S., Armitage, J.P., and Dow, J.M. (2010) Cell–cell signal-dependent dynamic interactions between HD-GYP and GGDEF domain proteins mediate virulence in *Xanthomonas campestris*. *Proc Natl Acad Sci USA* **107:** 5989–5994.

Ryan, R.P., Vorhoelter, F.-J., Potnis, N., Jones, J.B., Van Sluys, M.-A., Bogdanove, A.J., *et al*. (2011) Pathogenomics of *Xanthomonas*: understanding bacterium-plant interactions. *Nat Rev Microbiol* **9:** 344–355.

Ryan, R.P., McCarthy, Y., Kiely, P.A., O'Connor, R., Farah, C.S., Armitage, J.P., and Dow, J.M. (2012) Dynamic complex formation between HD-GYP, GGDEF and PilZ domain proteins regulates motility in *Xanthomonas campestris*. *Mol Microbiol* **86:** 557–567.

Rybtke, M.T., Borlee, B.R., Murakami, K., Irie, Y., Hentzer, M., Nielsen, T.E., *et al*. (2012) Fluorescence-based reporter for gauging cyclic di-GMP levels in *Pseudomonas aeruginosa*. *Appl Environ Microbiol* **78:** 5060–5069.

Sambrook, J., Fritsch, E.F., and Maniatis, T. (1989) *Molecular Cloning: A Laboratory Manual*, 2nd edn. New York: Cold Spring Harbor Laboratory Press.

Slater, H., Alvarez-Morales, A., Barber, C.E., Daniels, M.J., and Dow, J.M. (2000) A two-component system involving an HD-GYP domain protein links cell–cell signaling to pathogenicity gene expression in *Xanthomonas campestris*. *Mol Microbiol* **38:** 986–1003.

Trapnell, C., Williams, B.A., Pertea, G., Mortazavi, A., Kwan, G., van Baren, M.J., *et al*. (2010) Transcript assembly and quantification by RNA-Seq reveals unannotated transcripts and isoform switching during cell differentiation. *Nat Biotechnol* **28:** 511–515.

Trapnell, C., Hendrickson, D.G., Sauvageau, M., Goff, L., Rinn, J.L., and Pachter, L. (2012) Differential analysis of gene regulation at transcript resolution with RNA-Seq. *Nat Biotechnol* **31:** 46–53.

Wang, L.H., He, Y., Gao, Y., Wu, J.E., Dong, Y.H., He, C., *et al*. (2004) A bacterial cell–cell communication signal with cross-kingdom structural analogues. *Mol Microbiol* **51:** 903–912.

Supporting information

Additional supporting information may be found in the online version of this article at the publisher's web-site.